

Published in final edited form as:

Nature. 2012 November 15; 491(7424): 458–462. doi:10.1038/nature11540.

Serine is a natural ligand and allosteric activator of pyruvate kinase M2

Barbara Chaneton^{#1}, Petra Hillmann^{#2}, Liang Zheng¹, Agnès C.L. Martin², Oliver D.K. Maddocks¹, Achuthanunni Chokkathukalam³, Joseph E Coyle², Andris Jankevics^{3,4}, Finn P. Holding², Karen H. Vousden¹, Christian Frezza^{1,#}, Marc O'Reilly², and Eyal Gottlieb¹

¹Cancer Research UK, The Beatson Institute for Cancer Research, Switchback Road, Glasgow, G61 1BD, Scotland, United Kingdom ²Astex Pharmaceuticals, 436 Cambridge Science Park, Milton Road, Cambridge, CB4 0QA, United Kingdom ³Institute of Molecular, Cell and Systems Biology, College of Medical, Veterinary and Life Sciences, Joseph Black Building, B3.09, University of Glasgow, Glasgow, G12 8QQ, Scotland, United Kingdom ⁴Groningen Bioinformatics Centre, Groningen Biomolecular Sciences and Biotechnology Institute, University of Groningen, Groningen, The Netherlands.

These authors contributed equally to this work.

Abstract

Cancer cells exhibit several unique metabolic phenotypes that are critical for cell growth and proliferation. Specifically, they over-express the M2 isoform of the tightly regulated enzyme pyruvate kinase (PKM2), which controls glycolytic flux, and they are highly dependent on *de novo* biosynthesis of serine and glycine. Here we describe a novel rheostat-like mechanistic relationship between PKM2 activity and serine biosynthesis. We show that serine can bind to and activate human PKM2 and that following serine deprivation, PKM2 activity in cells is reduced. This reduction in PKM2 activity shifts cells to a fuel-efficient mode where more pyruvate is diverted to the mitochondria and more glucose derived carbon is channelled into serine biosynthesis to support cell proliferation.

Metabolic fluxes in cancer cells are different from those in non-transformed cells¹. In particular, a shift from oxidative phosphorylation to aerobic glycolysis has been demonstrated, which is promoted by the M2 isoform of pyruvate kinase (PK)². PKM2 catalyses the final step of glycolysis, converting phosphoenolpyruvate (PEP) to pyruvate (Supplementary Fig. 1). Interestingly, PKM2, which is the predominant isoform in cancer

Correspondence and requests for materials should be addressed to E.G. (e.gottlieb@beatson.gla.ac.uk) and M.O. (marc.oreilly@astx.com).

[#]Present address: MRC Cancer Cell Unit, Hutchison/MRC Research Centre, Hills Road Cambridge, CB2 0XZ, United Kingdom.

Author Contributions M.O. and E.G. conceived the project and wrote the manuscript with the help of B.C., P.H. and C.F. L.Z. B.C. and C.F. performed the LC-MS assay and analysed the raw data. A.C. and A.J. analysed the LC-MS data and identified the different isotopomers of each metabolite. A.C.L.M. performed the *in vitro* enzymatic activity, J.E.C. performed the ITC, M.O. generated the point mutant constructs, purified the proteins & solved the crystal structure. F.P.H. performed the LC-MS validation of the point mutant constructs. O.D.K.M. and K.H.V. performed, analysed and discussed the long-term serine and glycine starvation experiment. B.C. and P.H. generated and characterized the cell lines and performed all other experiments and data analysis. All the authors discussed the results and commented on the manuscript.

Supplementary Information available online Full Methods and any associated references are available in the online version of this paper. A figure summarising the main findings of this paper is available in Supplementary Figure 1.

Author information Atomic coordinates and structure factors for the PKM2 crystal structures have been deposited in the Protein Data Bank (PDB) accession code 4B2D

Declaration of competing financial interests E.G. is a consultant of Astex Pharmaceuticals

cells^{3,4}, has low basal enzymatic activity compared to the constitutively active splice-variant PKM1⁵. Another metabolic pathway recently demonstrated to be crucial for cancer cell survival is the serine biosynthesis pathway⁶⁻⁸. We investigated a potential mechanistic link between the two pathways in cancer cells, whereby a reduction of overall PK activity via the preferential expression of PKM2 would cause the build-up of glycolytic intermediates for channelling into the serine biosynthetic pathway. To test this hypothesis, we employed human colon carcinoma HCT116 cells, which predominantly express the PKM2 isoform (Fig. 1a and Supplementary Fig. 2). Two discrete shRNA pools were used to generate two independent HCT116-derived cell lines (shPKMa and shPKMb) in which the expression of both the PKM1 and PKM2 isoforms was simultaneously and stably silenced (Fig. 1a and Supplementary Fig. 2c). Despite achieving greater than 90 % reduction in PKM1/2 mRNA and protein levels compared to cells expressing non-targeting shRNA (shCntrl), no compensatory transcriptional induction of the PKL/R isoforms was observed in the shPKM cells (Supplementary Fig. 2). In line with this, liquid chromatography-mass spectrometry (LC-MS) analysis of the steady-state levels of metabolites revealed a 100-fold increase in PEP concentration in shPKM cells accompanied by ~50 % decrease in pyruvate levels, demonstrating a reduction in intracellular PK activity (Fig. 1b). The stable silencing of PKM1/2 in HCT116 cells did not alter cell proliferation rates or steady-state levels of ATP (Fig. 1c-d). In contrast, the proliferation rates of HT29 and SW620 colon cancer cells were more sensitive to PKM1/2 silencing (Supplementary Fig. 3a). Regardless of the effect on cellular proliferation rates, PKM1/2 silencing universally increased the oxygen consumption rates (OCR) by ~30 %, with a corresponding decrease in the extracellular acidification rates (ECAR), indicators of increased oxidative phosphorylation and decreased glycolysis, respectively (Supplemental Fig. 3b-c). Since PK catalyses an important ATP-producing step in glycolysis, the stability of intracellular ATP levels could be explained by this compensatory increase in oxidative phosphorylation in response to PKM1/2 silencing. Thus, despite the predominant expression of PKM2 in HCT116 cells, these cells still exhibit sufficient PK activity to convert PEP to pyruvate and to facilitate aerobic glycolysis.

Whilst PKM silencing caused a large increase in PEP concentration, pyruvate levels were decreased to a lesser extent (Fig. 1b). There are several possible explanations for this. Firstly, residual PKM could still generate pyruvate, albeit at a lower rate. Secondly, pyruvate can be synthesised from carbon sources other than glucose. Finally, pyruvate can also be generated from PEP via a PK-independent mechanism⁹, although this alternative pathway was not elevated in the knockdown cells (Supplementary Fig. 4).

In order to study the fate of glucose in PKM-inhibited cells shCntrl and shPKM cells were incubated in media containing uniformly ¹³C-labelled glucose (U-¹³C-glucose) and cells were extracted at different time points. Several glucose-derived metabolites were tracked by LC-MS (Fig. 2 and Supplementary Fig. 5), including pyruvate and PEP. The ratio between these two metabolites at an early time point after glucose labelling was validated as a reliable measure of PKM2 activity using an activator of PKM2 (Supplementary Fig. 5 and 6 and Supplementary discussion).

In the cytosol, pyruvate is metabolised to lactate by lactate dehydrogenase (LDH) and the resulting lactate contains three glucose-derived carbons. In addition, pyruvate is translocated to the mitochondria where it is oxidised and decarboxylated to acetyl-CoA which enters the tricarboxylic acid (TCA) cycle to form citrate, contributing two carbon atoms from glucose. When cells were incubated with U-¹³C-glucose, both glucose-derived lactate and citrate were detected by LC-MS (¹³C₃-Lactate and ¹³C₂-Citrate). Blocking PKM1/2 activity shifted the metabolism of glucose away from lactate production in the cytosol to citrate production in the mitochondria (Fig. 2 and Supplementary Fig. 5). Heavier isotopomers of citrate (particularly ¹³C₄-Citrate) were detected in cells incubated for a longer time (4 hours) with

U-¹³C-glucose, an indication of further oxidation and generation of citrate in the TCA cycle (Supplementary Fig. 7). These results are in line with the observed increase in oxygen consumption of shPKM cells (Supplementary Fig. 3).

An increased metabolic flux into the serine and glycine biosynthetic pathway was also observed in cells with reduced PK activity, as determined by the accumulation of glucose-derived ¹³C in these amino acids (Fig. 2 and Supplementary Fig. 5). This is the first direct evidence that low PK activity can drive serine and glycine biosynthesis, and demonstrates an important link between key metabolic processes observed in cancer, namely preferential PKM2 expression, aerobic glycolysis and serine biosynthesis. The relative contribution of glucose-derived carbons to serine and glycine is low (Supplementary Fig. 7), which is attributable to the presence of unlabelled serine and glycine in the growth media of the cells. Indeed, when cells were incubated for 12 hours in serine- and glycine-free media, more than 80 % of the intracellular serine and glycine was glucose-derived (Supplementary Fig. 8a). Nevertheless, *de novo* synthesis of serine and glycine in cells starved of these two amino acids was insufficient to recover their steady-state levels (Fig. 3a), indicating a rapid utilisation of newly-synthesised amino acids. Importantly, the absence of extracellular serine and glycine had a pronounced inhibitory effect on PK activity, as demonstrated by a 100 % increase in PEP and a 30 % decrease in pyruvate (Fig. 3a). Akin to PKM1/2 silencing, serine deprivation reduced cytosolic lactate production and increased mitochondrial citrate production by ~ 60 % (Fig. 3a). Moreover, cellular deprivation of serine and glycine for 12 hours followed by 30 minutes incubation with U-¹³C-glucose resulted in a 50 % decrease in the labelled pyruvate/PEP ratio (Fig. 3b). These data indicate that serine and glycine deprivation decreases PKM2 activity in cells, such that more glucose-derived carbon is channelled into serine and glycine biosynthesis.

PKM2 is a tightly regulated enzyme which responds not only to the availability of PEP and ADP substrates, but also to the upstream glycolytic metabolite fructose-1,6-bisphosphate (FBP) and to phosphorylation events¹⁰⁻¹⁴. Previous studies proposed that PK activity may be regulated by amino acids¹⁵⁻¹⁷. Therefore, the ability of serine or glycine to stimulate PKM2 in cells was tested. Serine hydroxymethyl transferase converts serine to glycine and *vice versa*, therefore cells were starved of both amino acids overnight prior to 30 minutes incubation with either serine or glycine. The cells incubated with serine or glycine showed an increase in the intracellular levels of the added amino acid only and the levels of the other amino acid were unaffected (Supplementary Fig. 8b). When serine- and glycine-starved cells were incubated for 30 minutes with serine together with U-¹³C-glucose, intracellular PK activity was increased relative to the starved cells. However, glycine did not stimulate intracellular PK activity (Supplementary Fig. 8c).

In order to substantiate the results observed in cells, recombinant human PKM2 activity was further analysed *in vitro*. Serine was demonstrated to activate recombinant PKM2 with a half maximal activation concentration (AC₅₀) of 1.3 mM (Fig. 4a), a level which is within the physiological range of intracellular serine concentrations (Fig. 1b). Isothermal titration calorimetry was used to determine the dissociation constant (K_d) of the PKM2-serine interaction as 0.20 mM (Fig. 4b) and the titration curve was consistent with a (1:1) PKM2-monomer: serine ratio. These results not only demonstrate direct interactions between serine and PKM2, they also suggest that the serine concentration required for such interactions is well within the physiological range of intracellular serine levels. In agreement with the results observed in cells, glycine could not directly activate PKM2 *in vitro* (Fig. 4a). Similarly to FBP, serine lowered the K_m of PKM2 for PEP 2.3-fold, effectively increasing the affinity of PKM2 for this substrate (Fig. 4c). Serine was found to be the only standard amino acid that could activate PKM2 (Supplementary Fig. 9a). A fragment-based crystallographic screen¹⁸ versus human PKM2 revealed the amino acids L-alanine, L-

cysteine, L-threonine and L-serine bound to a previously uncharacterised binding pocket on PKM2. Crystallographic soaking experiments revealed L-serine bound to PKM2, with a single L-serine molecule bound to each of the monomers comprising the PKM2 tetramer (Fig. 4d and Supplementary Tables 1-2). L-serine made multiple hydrogen bonding interactions with PKM2 (see Supplementary Fig. 9 and supplementary discussion). Additional interactions afforded by the serine side chain hydroxyl group rationalise the low affinity of glycine for PKM2 and may contribute to the unique ability of serine to activate PKM2¹⁶. The amino acid binding pocket was vacant in crystals not soaked with serine (Supplementary Fig. 9b).

Based on the above observations, a recombinant H464A PKM2 mutant was produced and demonstrated neither direct binding to, nor activation by, serine (Fig. 4b and e). These data confirm that the amino acid binding site identified in the soaking experiments is the only amino acid binding site on the PKM2 protein. Despite its inability to bind serine, the H464A PKM2 mutant was activated by FBP in a similar way to wild-type PKM2. Conversely, a S437Y mutant of PKM2, which cannot bind FBP¹⁹, was activated by serine (Fig. 4e-f). These results demonstrate that PKM2 is independently activated by either FBP or serine, and that, both molecules could contribute to PKM2 regulation in response to glucose and/or amino acid deprivation *in vivo*. PKM2 regulation by serine in tumours is important as the serine concentration in the blood is ~20-fold below that of glucose, hence under interrupted blood supply, a significant deficit in serine supply would occur. Serine is crucial for multiple metabolic pathways required for cell growth and proliferation, including phospholipid, purine and glutathione biosynthesis, as well as being a methyl source for single carbon metabolism. Additionally, serine levels are depleted at the periphery of solid tumours, hence *de novo* serine biosynthesis is critical for tumour growth^{20,21}.

The allosteric regulation of PK is associated with complex structural changes^{10,13,22}. Phosphorylation of Tyr105, adjacent to Arg106 in the serine binding pocket, has been shown to modulate PKM2 activity and FBP binding¹¹, and oxidation of Cys358, which is proximal to the serine binding pocket, inhibits PKM2²³ (Supplementary Fig. 9e). This suggests that the PKM2 serine binding pocket, and proximal residues, constitute a key structural regulatory node for PKM2.

The predominant isoform of PK in cancer cells is PKM2, however, the serine binding site identified here is conserved in PKM1 and PKL/R. Therefore, the possibility that serine may be a universal PK regulator was tested *in vitro*. PKM1 demonstrated a high degree of basal activity in the absence of exogenous activators, and was refractory to both FBP and serine activation (Fig. 4g). In contrast, PKL/R was completely inactive in its basal state and was robustly activated by FBP. Surprisingly, PKL/R was not activated by serine (Fig. 4h). These results suggest that only PKM2-expressing cells can respond to changes in serine availability and support shuttling of glucose-derived carbon into serine biosynthesis upon serine deprivation.

This work provides a new understanding of the relationship between glucose and amino acid metabolism. Serine biosynthesis is an anabolic pathway required for growth and proliferation²⁴. However, it recruits carbon away from the energy production pathway of glucose utilisation. Here, for the first time, we present an elucidation of the mechanism that tightly controls the metabolic bifurcation of glucose-derived carbon. The control of PKM2 activity through serine availability provides a rheostat-like mechanism. When serine is abundant, PKM2 is fully active enabling the maximal use of glucose via glycolysis. However, when the steady-state levels of serine drop below a critical point, an immediate attenuation of PKM2 activity occurs. This enables the fast shuttling of glucose-derived carbon to serine biosynthesis, compensating for the serine shortfall and enabling growth and

proliferation in the absence of these amino acids (Supplementary Fig. 1). Finally, by activating PKM2, serine supports aerobic glycolysis and lactate production, events that are critical for cancer cell growth and survival.

Full Methods

Cell culture

HCT116 and HT29 colon cancer cells were maintained at 37°C and 5% CO₂ in high glucose DMEM (21969-035, Invitrogen, Paisley, UK) supplemented with 10% FBS and 2 mM L-Glutamine. SW620 colon cancer cells were maintained at 37°C and 5% CO₂ in RPMI (12633-020, Invitrogen, Paisley, UK) supplemented with 20% FBS and 2 mM L-Glutamine. Stable PKM1/2 knockdown and control cell lines were cultured in the same media containing additional 2 µg/ml puromycin.

Stable PKM1/2 silencing

HCT116, SW620 and HT29 cells were infected with control shRNA (shCntrl) (sc-108080) or PKM1/2 shRNA (shPKM) (sc-62820) lentiviral particles (Santa Cruz Biotechnology, Santa Cruz, CA, USA) according to the manufacturer's instructions. Infected cells were selected using 6 µg/ml puromycin and shPKM clones were analysed for PKM1 and PKM2 expression levels using Western blot analysis and qPCR. A different set of plasmids containing PKM1/2 shRNA (shPKMa) was bought from Openbiosystems TRCN0000037610 and TRCN0000037611. **pLKO** scramble shRNA (Openbiosystems) was used as a control (shCntrl). HCT116 cells were infected with both **pLKO-shPKM1/2** or **pLKO-shSCR** and selected using 2 µg/ml puromycin for 2 weeks and PKM1/2 silenced clones were analysed for PKM1 and PKM2 expression levels using Western blot analysis and qPCR.

mRNA extraction and qPCR analyses

4×10⁵ cells were plated in a 6 well plate and were lysed after 2 days in RLT buffer (Qiagen, West Sussex, UK). Lysates were passed through QiaShredder columns (Qiagen, West Sussex, UK) and mRNA was isolated using the RNAeasy kit (Qiagen, West Sussex, UK) following the manufacturer's instructions. RNA was quantified and quality controlled using an Eppendorf Biophotometer and Eppendorf single sealed cuvettes, UVette (Eppendorf UK Limited, Endurance House, UK). For PCR analyses 1 µg of mRNA was retro-transcribed into cDNA using High Capacity RNA-to-cDNA (AB, Life Technologies Corporation Carlsbad, California). In brief, 0.5 µM primers, 1X Fast SYBR Green Master mix (AB, Life Technologies Corporation Carlsbad, California) and 1 µL of a 1:10 dilution of cDNA in a final volume of 20 µL were used. Real-time PCR was performed on the 7500 Fast Real-Time PCR System (Life Technologies Corporation Carlsbad, California) and expression levels of the indicated genes were calculated using the $\Delta\Delta C_t$ method by the appropriate function of the software using actin as calibrant. The PCR program was: 20 seconds at 95°C followed by 40 cycles of 3 seconds at 95°C and 30 seconds at 60°C. Finally the melting curve was performed, which was used to confirm the presence of single PCR products. Primers are as follows: β -actin-Forward Primer: 5'-TCCATCATGAAGTGTGACGT-3'; β -actin-Reverse Primer: 5'-TACTCCTGCTTGCTGATCCAC-3'; PKM1-Forward Primer: 5'-GAGGCAGCCATGTTCCAC-3'; PKM1-Reverse Primer: 5'-TGCCAGACTCCGTCAGAACT-3'; PKM2- Forward Primer: 5'-CAGAGGCTGCCATCTACCAC-3'; PKM2- Reverse Primer: 5'-CCAGACTTGGTGAGGACGAT-3'. PKL Forward Primer: 5'-CTGGTGATTGTGGTGACAGG-3' PKL Reverse Primer: 5'-TGGGCTGGAGAACGTAGACT-3' PKR Forward Primer: 5'-caattggcattgaaagtgg-3' PKR Reverse Primer: 5'-cctgtaccacaatcaccag-3'

Immunoblotting

4×10^5 cells were plated in a 6 well plate and were lysed after 2 days in RIPA buffer (150 mM sodium chloride, 1.0% NP-40, 0.5% sodium deoxycholate, and 50 mM Tris, pH 8.0) supplemented with a 1:100 dilution of the protein inhibitors cocktail (Sigma, Gillingham, UK). Protein concentration was determined using the Bicinchoninic Acid Assay (Thermoscientific, Waltham, MA) using BSA as standard (Thermoscientific, Waltham, MA). Equal amounts of protein were loaded into a 12% SDS-PAGE gels and electrophoretically separated using Tris-Glycine SDS running buffer. After SDS-PAGE, proteins were transferred onto 0.22 μ m nitrocellulose (Millipore, Billerica, MA) and probed with antibodies, all at 1:1000 dilution in 5% non-fat milk. PKM1 antibody was custom-made by PolyPeptide Laboratories (Strasburg, France) using the following peptide sequence: CLVRASSHSTDLMEAMAMGS. The PKM2 (cat #3198) and PKM1/2 (#3186) antibodies were purchased from Cell Signaling Technology (Danvers, MA, USA). The anti-actin antibody (mouse monoclonal AC-40) was purchased from Sigma (Gillingham, UK). For detection, membranes were incubated with either donkey-anti rabbit (926 32213) or donkey-anti mouse (926 32212) secondary antibodies purchased from Licor, all at 1:1000 dilution in TBS Tween 0.1%. The infrared scanning was performed using the Licor Odyssey scanner, Channel 800, Brightness: 50, Contrast: 50, Sensitivity: auto, resolution: 169.492 micron, Pixel area: 0.02873, Intensity: 5 and acquired using Odyssey software version 3. Images were then exported as TIFF and cropped using Adobe Photoshop CS4.

Cell Proliferation

shPKM and control HCT116, HT29 or SW620 cells were seeded into a 96-well plate at a density of 1000 cells/well in 200 μ l of DMEM containing 2% FBS. On days 4 to 8 after seeding 20 μ l of Alamar Blue solution (life technologies, Paisley, UK) were added to each well measured. Cells were incubated for 6 hours and fluorescence was measured using 535 nm excitation and 590 nm emission wavelengths.

ATP levels

6×10^5 cells were seeded on a 6 well plate the day before the experiment. Cells were then washed twice with PBS in order to remove dead cells, and then lysed using the ATP-release buffer (Sigma, Gillingham, UK). ATP was then measured using a luciferase-based assay according to the manufacturer's instructions using the adenosine 5'-triphosphate (ATP) bioluminescent somatic cell assay kit FLASC (Sigma). Values were normalised to the total protein content of the cell lysate as measured by BCA assay (Thermoscientific, Waltham, MA) using BSA as standard.

Measurement of oxygen consumption rate (OCR) and extracellular acidification rate (ECAR)

3×10^4 cells were plated onto XF24 plates in DMEM (10% FBS, 2 mM Glutamine) (Seahorse Bioscience, North Billerica, MA) and incubated at 37°C, 5% CO₂ overnight. The medium was then replaced with 675 μ L of unbuffered assay media (Seahorse Bioscience, North Billerica, MA) supplemented with 2 mM glutamine, 25 mM glucose and 2% FBS (pH was adjusted to 7.4 using sodium hydroxide 0.5 mM) and cells were then placed at 37°C in a CO₂-free incubator for 30 minutes. Basal OCR and ECAR were recorded using the XF24 plate reader. At the end of the experiment 1 μ M antimycin A was added in order to measure mitochondria-independent oxygen consumption. Each measurement cycle consisted of 3 minutes mixing, 3 minutes waiting and 4 minutes measuring. OCR and ECAR were normalised to cell number. To obtain the mitochondrial-dependent OCR, only antimycin A-sensitive respiration was used. Homogeneous plating and cell count were assessed by fixing

the cells with 10% trichloroacetic acid for 1 hour at 4°C and then staining the fixed cells with 0.47% solution of Sulforhodamine B (SRB) (Sigma, Gillingham, UK).

Quantification of intra and extracellular metabolites by the Standard Addition method

1×10^6 cells were plated onto 6 cm plates in triplicates and cultured in standard medium (DMEM, 10% FBS, 2 mM glutamine). Two additional plates were grown as counter plates. The medium was replaced after 24 hours by 10 ml of fresh standard medium, and cells were incubated for another 24 hours before extraction (as described in the following section). Standard compounds were weighed separately and dissolved together in water to make solution A (where each metabolite has a concentration between 1 mM and 10 mM). 1 ml of solution A was added to 49 ml of dilution solvent (50:50 acetonitrile: water) to make stock solution B (where each metabolite had a concentration between 20 μ M and 200 μ M). For quantification, cells or media extracts (200 μ l) were mixed with 800 μ l of dilution solvent, containing 0, 4, 20, 100, 300 or 500 μ l of stock solution B. Dilutions were analysed by LC-MS. The concentration of each metabolite in the extract was calculated according to the linear regression fit²⁴. All dilution series were performed in triplicates using 3 biological replicates.

Measurement of ¹³C-labelled metabolites by LC-MS

4×10^5 cells were plated onto 6 well plates and cultured in standard medium for 24 hours. The medium was then replaced by 2 ml of fresh medium containing 5 mM unlabelled glucose and 3 hours later 5 mM of U-¹³C-glucose (Cambridge Isotope Laboratories, Inc) was added; alternatively, medium was replaced by 2 ml of fresh medium with U-¹³C-glucose only. Cells were incubated for the indicated time prior to extraction. For extraction, cells were washed twice in PBS and metabolites were extracted on a dry ice/methanol bath in a 50:30:20 ratio of methanol:acetonitrile:water and quickly scraped. The insoluble material was spun down in a cooled centrifuge at 16000g for 15 minutes at 0°C and the supernatant was collected for subsequent LC-MS analysis. The volume of extraction solution was calculated according to cell number and, extrapolated using a “counter dish” cultured under the same experimental conditions as the sample dishes. A volume of 1 ml of extraction solutions per 2×10^6 cells was used. Metabolites were separated using a liquid chromatography system. A ZIC-pHILIC column (4.6 mm \times 150 mm, guard column 4.6 mm \times 10 mm, Merck, Germany) was used for LC separation using gradient elution with a solution of 20 mM ammonium carbonate, with 0.1% ammonium hydroxide, and acetonitrile. Detection of metabolites was performed using a Thermo Scientific Exactive high resolution mass spectrometer with electrospray (ESI) ionization, examining metabolites in both positive and negative ion modes, over the mass range of 75-1000 m/z.

2D gel electrophoresis

shPKM and control HCT116 cells were lysed precipitated and resuspended as described in Vander Heiden et al, 2010⁹. IEF was performed using ZOOM strips pH 3-10NL according to the manufacturer’s instructions (Invitrogen). After IEF strips were equilibrated in buffer containing 10 mg/ml DTT and subsequently in buffer containing 25 mg/ml iodoacetamide prior to SDS-PAGE. As negative control, shPKM HCT116 cells were lysed and precipitated in acetone and the pH adjusted to pH5 by the addition of 1% acetic acid. This removed any acid labile phosphates such as phospho-Histidine. PGAM1 and its phosphorylated forms were detected by Western blot using goat anti-PGAM1 (Novus) 1:1000 and Donkey anti-Goat (Licor) 1:1000 antibodies.

PKM2 Activator

Cells were treated for 1 hour with 20 μM of the commercially available PKM2 activator (r 1-(3-Chloro-5-trifluoromethyl-pyridin-2-yl)-1H-pyrrole-2-sulfonic acid p-tolylamide, indicated in the manuscript as Cmpd1)²⁵ or with vehicle as control. Both were incubated in media containing 25 mM U-¹³C–glucose for the indicated time.

In vitro Measurement of PK Activity

PKM2 was expressed and purified as described in the “PKM2 X-ray Crystallography” section. Rabbit muscle PKM1 was obtained from Sigma; PKL/R was purchased from Abcam. Enzyme activity was measured *in vitro* with a coupled assay quantifying levels of ATP using luminescent Kinase-Glo Plus reagent (Promega) as described previously²⁶ with some modifications. Measurements were performed in the presence of 50 mM Tris pH 7.5, 100 mM KCl, 10 mM MgCl₂, 200 μM PEP, 200 μM ADP, 3% DMSO and either 4 nM PKM2, 4 nM PKM1 or 10 nM PKL/R. Reactions (25 μL) were incubated for 20 minutes on a shaker before addition of 25 μL Kinase-Glo Plus reagent, as per the manufacturer’s instructions. Luminescence was read with a PHERAstar (BMG LABTECH). The signal was normalised to the no enzyme controls. Activation curves were fitted to a four-parameter logistic equation and K_m curves were fitted to a Michaelis-Menten equation using Prism 5 (GraphPad).

Isothermal Titration Calorimetry (ITC)

ITC experiments were performed on a MicroCal VP-ITC at 25°C in a buffer comprising 50 mM Tris, 100 mM KCl, 10 mM MgCl₂ and 1 mM TCEP at pH 7.5. For titrations the L-serine concentration was 5 mM in the injection syringe and the PKM2 concentration was 28 μM in the sample cell. The protein concentration refers to the monomer. PKM2 was incubated for 30 minutes with an excess of FBP (200 μM) prior to the L-serine titration performed in the presence of FBP. The K_d value for L-serine binding was significantly higher than the PKM2 concentration used, making it difficult to accurately determine the stoichiometry value. Therefore, the stoichiometry parameter was fixed at 1 for the purpose of data analysis using the single site binding model in Origin 7.0.

PKM2 X-ray Crystallography

A publically available human PKM2 expression construct was obtained from the Structural Genomics Consortium (SGC). His₆-hPKM2 was purified using NiNTA affinity capture and Hiload Superdex 16/60 S75 size exclusion chromatography. hPKM2 was crystallised using hanging drop vapour diffusion. Protein solution 10 mg/ml, 25 mM Tris/HCl pH 7.5, 0.1 M KCl, 5 mM MgCl₂, 10% (v/v) glycerol was mixed in a (1:1) ratio with reservoir solution containing 0.1 M KCl, 0.2 M ammonium tartrate, 24% (w/v) PEG3350. Crystals were soaked overnight in a solution containing 30 mM L-Serine, cryo protected and flash frozen in liquid N₂. X-ray diffraction data were collected from a single crystal at 100K at Beamline-I03 at the Diamond Light Source. Diffraction data were processed using XDS AutoPROC from Global Phasing and SCALA (CCP4)²⁷. Molecular replacement was performed using model 3H6O (SGC) in CSEARCH²⁸ and maximum likelihood refinement carried out using a mixture of automated (see²⁹ & refs therein) and manual refinement protocols employing Refmac (CCP4) and AutoBuster from Global Phasing. Ligand fitting was performed using Autosolve²⁸ and manual rebuilding. Simulated annealing was not employed. The four PKM2 monomers comprising the tetramer in the asymmetric unit were refined as independent entities, but NCS restraints were imposed in AutoBuster using the ‘ncsauto’ command. Refinement of the structure in the absence of NCS restraints gave (Rf=23.7, R=17.7) and with ‘ncsauto’ gave (Rf=22.7, R=17.9), showing a small, but significant, reduction in Rf using ‘ncsauto’ restraints. At the ‘effective resolution’ of 2.36Å

there are ~86000 unique reflections. The refinement included ~16600 non-hydrogen atoms. B-factors were refined isotropically giving a total of ~66500 parameters for all non-hydrogen atoms in the PKM2 tetramer. The four serine molecules were refined as independent ligands. Details of ligand occupancies, B-factors *etc* are tabulated in the crystallographic data tables (Supplementary Tables 1-2)³⁰⁻³³.

PKM2 Mutagenesis

hPKM2 point mutant constructs were generated using a Stratagene QuikChange II site directed mutagenesis kit (#200524). PCR protocols were as defined in the product manual. The following forward DNA primers, and their reverse complemented primer counterparts, were used for the mutagenesis reactions (sequence of mutated bases shown in uppercase bold): H464A: 5'gctcgtcaggcc**GC**cctgtaccgtggc3', S437Y: 5'accaagtctggcaggt**At**gctcaccaggtgg3'. Primers were purchased from Sigma (UK). The previously described SGC hPKM2 construct was used as the DNA template within the PCR reactions. The presence of the point mutations was confirmed by DNA sequencing of the DNA constructs (Beckman Coulter Genomics Inc., Takeley, UK) and in-house LC-MS of the purified recombinant proteins. The mutant proteins were expressed and purified identically to the wild type protein.

Statistical analyses

The data (mean \pm s.e.m.) are representative of 3-5 independent experiments, performed in technical triplicates if not differently indicated. Data were analysed and presented with Graphpad Prism 5.01 software (GraphPad Software Inc, CA, USA).

Data Processing

The data processing workflow started by first converting the vendor specific raw data files from the mass spectrometer into the mzXML open data format³⁴, using the msconvert utility from the ProteoWizard Library and Tools collection³⁵ (<http://proteowizard.sourceforge.net/>). The set of all chromatographic peaks in each of the converted raw files were then extracted using the CentWave³⁶ feature detection algorithm from XCMS³⁷. The resulting data were stored in the PeakML file format³⁸, and the rest of the processing was handled by the scriptable mass spectrometry data processing tool mzmach.R³⁹ (<http://mzmach.sourceforge.net/>).

The next step in the workflow involved aligning and combining the chromatographic features between biological replicates of a single sample. The PeakML files thus created were subjected to an additional filtering procedure to discard all peaks that were not reproducibly detected in all biological replicates involved. Chromatographic peaks of individual samples were then aligned together based on their retention time and m/z values, and combined into a single PeakML file. Peak sets that do not include peaks from every sample were filled in by extracting ion chromatograms within the retention time and mass window of the corresponding peak set directly from the raw data files. From these peak sets, only those that had more peaks than the number of replicates minus one were selected for further analysis. Putative identification of the peak sets were made by matching the detected masses to that of the compounds relevant to this study. Isotope peaks were extracted by identifying the peaks that fell in the retention time window of the identified unlabelled peak and correspond to the estimated mass window (2 ppm) of the isotope. All isotope identification and quantification of the ratios were performed by the PeakML.Isotope.TargettedIsotopes() function of the mzmach.R library. Detailed documentation and tutorials for which are available at http://mzmach.sourceforge.net/isotopes_targetted.html.

Supplementary Material

Refer to Web version on PubMed Central for supplementary material.

Acknowledgments

The work performed at the Beatson Institute for Cancer Research was supported by Cancer Research UK. We thank Neil Thompson, Nicola Wallis and Michelle Jones for comments provided during manuscript preparation. We would also like to thank the Structural Genomics Consortium (SGC) for providing us with the PKM2 expression plasmid from their collection. We thank Ayala King for excellent editorial work.

References

1. Tennant DA, Duran RV, Gottlieb E. Targeting metabolic transformation for cancer therapy. *Nat Rev Cancer*. 2010; 10:267–277. doi:nrc2817 [pii] 10.1038/nrc2817. [PubMed: 20300106]
2. Christofk HR, et al. The M2 splice isoform of pyruvate kinase is important for cancer metabolism and tumour growth. *Nature*. 2008; 452:230–233. doi:nature06734 [pii] 10.1038/nature06734. [PubMed: 18337823]
3. Altenberg B, Greulich KO. Genes of glycolysis are ubiquitously overexpressed in 24 cancer classes. *Genomics*. 2004; 84:1014–1020. doi:S0888-7543(04)00227-7 [pii] 10.1016/j.ygeno.2004.08.010. [PubMed: 15533718]
4. Mazurek S, Boschek CB, Hugo F, Eigenbrodt E. Pyruvate kinase type M2 and its role in tumor growth and spreading. *Semin Cancer Biol*. 2005; 15:300–308. doi:S1044-579X(05)00026-X [pii] 10.1016/j.semcancer.2005.04.009. [PubMed: 15908230]
5. Yamada K, Noguchi T. Nutrient and hormonal regulation of pyruvate kinase gene expression. *Biochem J*. 1999; 337(Pt 1):1–11. [PubMed: 9854017]
6. Possemato R, et al. Functional genomics reveal that the serine synthesis pathway is essential in breast cancer. *Nature*. 2011; 476:346–350. doi:10.1038/nature10350 nature10350 [pii]. [PubMed: 21760589]
7. Locasale JW, et al. Phosphoglycerate dehydrogenase diverts glycolytic flux and contributes to oncogenesis. *Nat Genet*. 2011; 43:869–874. doi:10.1038/ng.890 ng.890 [pii]. [PubMed: 21804546]
8. Pollari S, et al. Enhanced serine production by bone metastatic breast cancer cells stimulates osteoclastogenesis. *Breast Cancer Res Treat*. 2011; 125:421–430. doi:10.1007/s10549-010-0848-5. [PubMed: 20352489]
9. Vander Heiden MG, et al. Evidence for an alternative glycolytic pathway in rapidly proliferating cells. *Science*. 2010; 329:1492–1499. doi:329/5998/1492 [pii] 10.1126/science.1188015. [PubMed: 20847263]
10. Dombrackas JD, Santarsiero BD, Mesecar AD. Structural basis for tumor pyruvate kinase M2 allosteric regulation and catalysis. *Biochemistry*. 2005; 44:9417–9429. doi:10.1021/bi0474923. [PubMed: 15996096]
11. Hitosugi T, et al. Tyrosine phosphorylation inhibits PKM2 to promote the Warburg effect and tumor growth. *Sci Signal*. 2009; 2:ra73. doi:2/97/ra73 [pii] 10.1126/scisignal.2000431. [PubMed: 19920251]
12. Christofk HR, Vander Heiden MG, Wu N, Asara JM, Cantley LC. Pyruvate kinase M2 is a phosphotyrosine-binding protein. *Nature*. 2008; 452:181–186. doi:nature06667 [pii] 10.1038/nature06667. [PubMed: 18337815]
13. Ashizawa K, Willingham MC, Liang CM, Cheng SY. In vivo regulation of monomer-tetramer conversion of pyruvate kinase subtype M2 by glucose is mediated via fructose 1,6-bisphosphate. *J Biol Chem*. 1991; 266:16842–16846. [PubMed: 1885610]
14. Chaneton B, Gottlieb E. Rocking cell metabolism: revised functions of the key glycolytic regulator PKM2 in cancer. *Trends in biochemical sciences*. 2012 doi:10.1016/j.tibs.2012.04.003.
15. Spellman CM, Fottrell PF. Similarities between pyruvate kinase from human placenta and tumours. *FEBS Lett*. 1973; 37:281–284. doi:0014-5793(73)80478-8 [pii]. [PubMed: 4763335]

16. Eigenbrodt E, Leib S, Kramer W, Friis RR, Schoner W. Structural and kinetic differences between the M2 type pyruvate kinases from lung and various tumors. *Biomed Biochim Acta*. 1983; 42:S278–282. [PubMed: 6326772]
17. Ye J, et al. Pyruvate kinase M2 promotes de novo serine synthesis to sustain mTORC1 activity and cell proliferation. *Proceedings of the National Academy of Sciences of the United States of America*. 2012; 109:6904–6909. doi:10.1073/pnas.1204176109. [PubMed: 22509023]
18. Davies TG, Tickle IJ. Fragment screening using X-ray crystallography. *Top Curr Chem*. 2012; 317:33–59. doi:10.1007/128_2011_179. [PubMed: 21678136]
19. Allali-Hassani A, et al. A survey of proteins encoded by non-synonymous single nucleotide polymorphisms reveals a significant fraction with altered stability and activity. *Biochem J*. 2009; 424:15–26. doi:BJ20090723 [pii] 10.1042/BJ20090723. [PubMed: 19702579]
20. Medina MA, Marquez J, Nunez de Castro I. Interchange of amino acids between tumor and host. *Biochem Med Metab Biol*. 1992; 48:1–7. [PubMed: 1524866]
21. Marquez J, Sanchez-Jimenez F, Medina MA, Quesada AR, Nunez de Castro I. Nitrogen metabolism in tumor bearing mice. *Arch Biochem Biophys*. 1989; 268:667–675. [PubMed: 2913952]
22. Mattevi A, Bolognesi M, Valentini G. The allosteric regulation of pyruvate kinase. *FEBS Lett*. 1996; 389:15–19. doi:0014-5793(96)00462-0 [pii]. [PubMed: 8682196]
23. Anastasiou D, et al. Inhibition of Pyruvate Kinase M2 by Reactive Oxygen Species Contributes to Antioxidant Responses. *Science*. 2011 doi:science.1211485 [pii] 10.1126/science.1211485.

Methods References

24. de Koning TJ, et al. L-serine in disease and development. *Biochem J*. 2003; 371:653–661. doi: 10.1042/BJ20021785 BJ20021785 [pii]. [PubMed: 12534373]
24. Luo B, Groenke K, Takors R, Wandrey C, Oldiges M. Simultaneous determination of multiple intracellular metabolites in glycolysis, pentose phosphate pathway and tricarboxylic acid cycle by liquid chromatography-mass spectrometry. *J Chromatogr A*. 2007; 1147:153–164. doi:S0021-9673(07)00290-7 [pii] 10.1016/j.chroma.2007.02.034. [PubMed: 17376459]
25. Salituro, FG.; Saunders, JO. Therapeutic compositions and related methods of use. patent WO/2010/118063. 2010. p. 52
26. Boxer MB, et al. Evaluation of substituted N,N'-diarylsulfonamides as activators of the tumor cell specific M2 isoform of pyruvate kinase. *J Med Chem*. 2010; 53:1048–1055. doi:10.1021/jm901577g. [PubMed: 20017496]
27. Collaborative Computational Project. Number 4. *Acta Cryst*. 1994; D50:760–763.
28. Mooij WT, et al. Automated protein-ligand crystallography for structure-based drug design. *ChemMedChem*. 2006; 1:827–838. doi:10.1002/cmcd.200600074. [PubMed: 16902937]
29. Davies TG, Tickle IJ. Fragment screening using X-ray crystallography. *Top Curr Chem*. 2012; 317:33–59. doi:10.1007/128_2011_179. [PubMed: 21678136]
30. Brunger AT. Free R value: a novel statistical quantity for assessing the accuracy of crystal structures. *Nature*. 1992; 355:472–475. [PubMed: 18481394]
31. Diederichs K, Karplus PA. Improved R-factors for diffraction data analysis in macromolecular crystallography. *Nature structural biology*. 1997; 4:269–275.
32. Weiss MS, H. R. On the use of the merging R-factor as a quality indicator for X-ray data. *J. Appl. Cryst*. 1997:203–205.
33. Weiss MS. Global indicators of X-ray data quality. *J.Appl.Cryst*. 2001:130–135.
34. Pedrioli PG, et al. A common open representation of mass spectrometry data and its application to proteomics research. *Nat Biotechnol*. 2004; 22:1459–1466. doi:nbt1031 [pii] 10.1038/nbt1031. [PubMed: 15529173]
35. Kessner D, Chambers M, Burke R, Agus D, Mallick P. ProteoWizard: open source software for rapid proteomics tools development. *Bioinformatics*. 2008; 24:2534–2536. doi:btn323 [pii] 10.1093/bioinformatics/btn323. [PubMed: 18606607]

36. Tautenhahn R, Bottcher C, Neumann S. Highly sensitive feature detection for high resolution LC/MS. *BMC Bioinformatics*. 2008; 9:504. doi:1471-2105-9-504 [pii] 10.1186/1471-2105-9-504. [PubMed: 19040729]
37. Smith CA, Want EJ, O'Maille G, Abagyan R, Siuzdak G. XCMS: processing mass spectrometry data for metabolite profiling using nonlinear peak alignment, matching, and identification. *Anal Chem*. 2006; 78:779–787. doi:10.1021/ac051437y. [PubMed: 16448051]
38. Fernandez CA, Des Rosiers C, Previs SF, David F, Brunengraber H. Correction of ¹³C mass isotopomer distributions for natural stable isotope abundance. *J Mass Spectrom*. 1996; 31:255–262. [PubMed: 8799277]
39. Scheltema RA, Jankevics A, Jansen RC, Swertz MA, Breitling R. PeakML/mzMatch: a file format, Java library, R library, and tool-chain for mass spectrometry data analysis. *Anal Chem*. 2011; 83:2786–2793. doi:10.1021/ac2000994. [PubMed: 21401061]

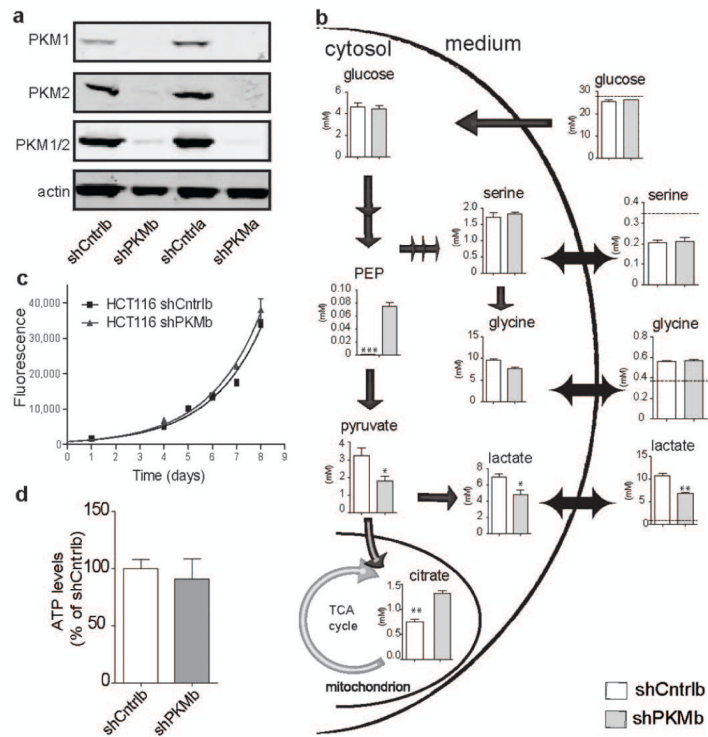


Figure 1. Characterisation of PKM1/2-silenced HCT116 cells

a, Protein levels of PKM1 and PKM2 in the indicated cell lines were detected by Western blot. Actin was used as a loading control. **b**, Quantified intracellular metabolite concentrations and the uptake or secretion of extracellular metabolites in control and shPKM HCT116 cells. For extracellular metabolites, the dashed line indicates the initial levels in the medium, while the graph represents the levels after 24 hours incubation. **c**, The proliferation rate of the indicated cell lines was measured by an Alamar Blue assay. **d**, Intracellular ATP levels of the indicated cells normalised to protein concentration in the cell extracts. All results are from 3 independent cultures and are presented as mean \pm s.e.m. * = $P < 0.05$, ** = $P < 0.01$, *** = $P < 0.001$.

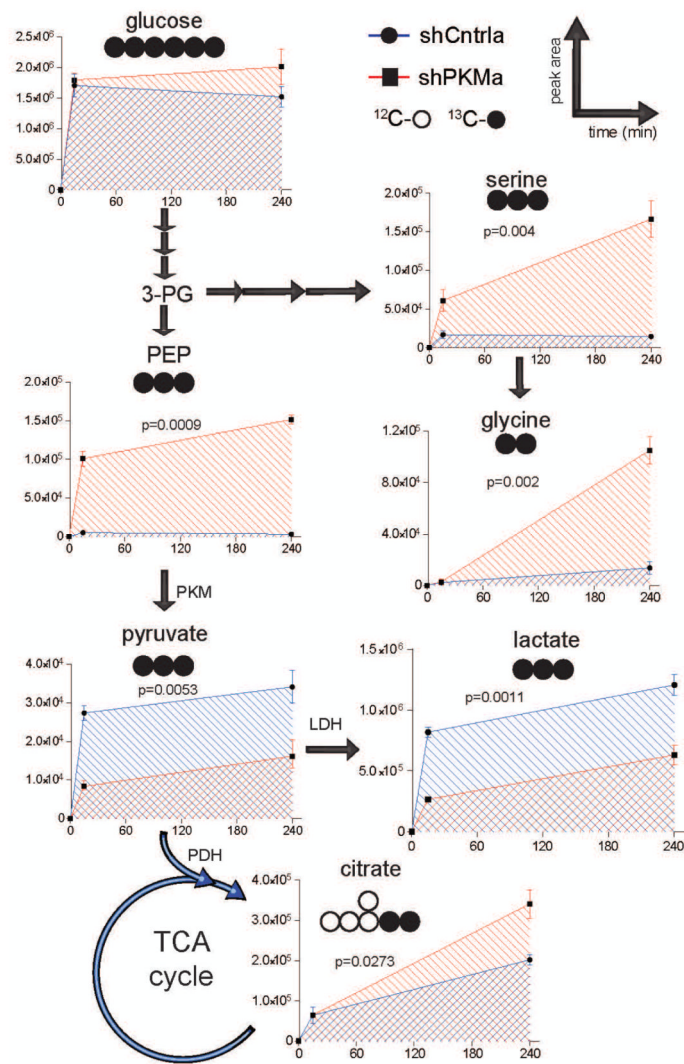


Figure 2. The effect of PKM1/2 silencing on glycolytic flux

HCT116 shCntrl and shPKM cells were incubated with U- ^{13}C -glucose and the abundance of the main glucose-derived isotopomer of the indicated metabolites was analysed at the indicated time points. The cumulative intensities of each labelled metabolite analysed in each cell line are presented in blue (shCntrl) or red (shPKM). The white and black circles under each metabolite illustrate ^{12}C - and ^{13}C -labelling, respectively. All metabolic quantifications were performed from 3 independent cultures and presented as mean \pm s.e.m. 3-PG, 3-phosphoglycerate; PEP, phosphoenolpyruvate; PKM, pyruvate kinase; PDH, pyruvate dehydrogenase; LDH, lactate dehydrogenase; TCA, tricarboxylic acid. P values at 4 hrs are shown when significant.

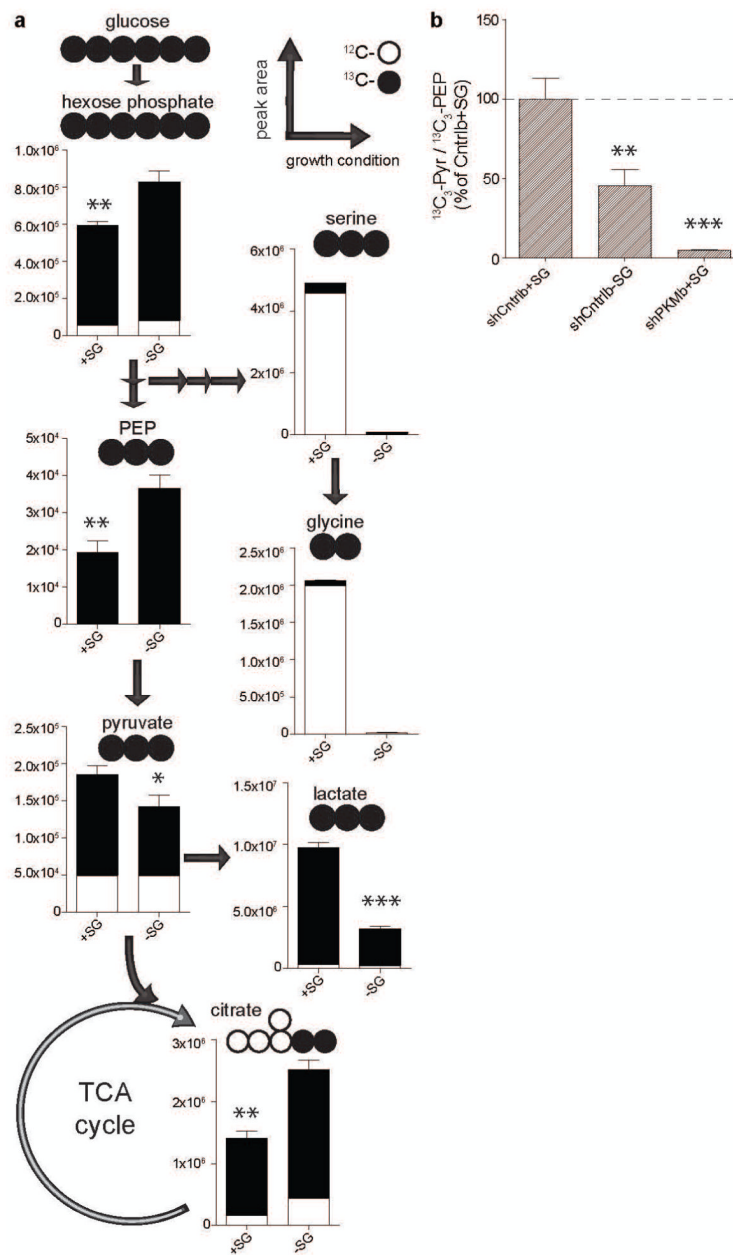


Figure 3. Serine and glycine deprivation changes glucose metabolism

a, Parental HCT116 cells were incubated for 12 hours with U-¹³C-glucose in the presence (+SG) or absence (–SG) of serine and glycine. The abundance of the main glucose-derived isotopomer (black bars) and the unlabelled fraction (white bars) of the indicated metabolites were analysed. The circles represent the isotopomer distribution of each individual metabolite. **b**, PK activity is represented as the ratio between glucose-derived (¹³C₃-) pyruvate and PEP, 30 minutes after labelling with U-¹³C-glucose in the presence or absence of serine and glycine in the indicated cell lines. Results were normalised to shCntrl +SG. PEP, phosphoenolpyruvate. All results are from 3 independent cultures and they are presented as mean ± s.e.m. * = P < 0.05, ** = P < 0.01, *** = P < 0.001.

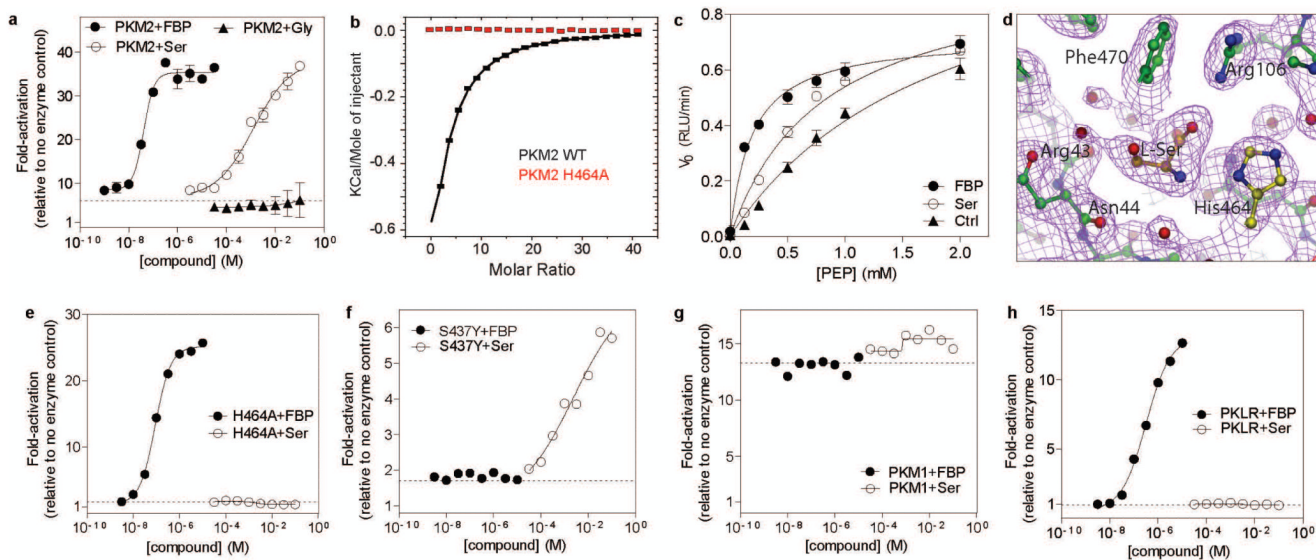


Figure 4. Serine is an allosteric activator of PKM2

a, *In vitro* activity of recombinant human PKM2 was analysed in the presence of increasing concentrations of FBP (●), serine (○) or glycine (▲). **b**, Serine binding to PKM2 wild-type or H464A mutant was measured by isothermal titration calorimetry. The K_d of serine for wild-type PKM2 was measured as 200 μ M. No serine binding to H464A PKM2 was detected. **c**, The initial PKM2 reaction (V_0) was measured at different PEP concentrations in the presence of 50 μ M FBP (●), 100 mM Serine (○) or vehicle (▲). K_m values for PEP were determined as 1.9 mM, 0.81 mM and 0.19 mM in the presence of vehicle, serine and FBP, respectively. For **a** and **c**, results are from 3 independent experiments and are presented as mean \pm s.e.m. FBP, fructose 1,6-bisphosphate. **d**, 2.3 \AA 2Fo-Fc map (purple) contoured at 1 σ for the final, refined, structure of L-ser (orange) bound to PKM2 (green). The side chain of His464, which was subsequently mutated to alanine, is shown in yellow. A detailed schematic representation of the L-ser interactions is shown in Supplementary Fig. 9d. **e-f**, *In vitro* activity of PKM2 mutants H464A (**e**) and S437Y (**f**) was analysed in the presence of increasing concentrations of FBP (●) or Serine (○). **g-h**, *In vitro* activity of PKM1 (**g**) and PKLR (**h**) was analysed in the presence of increasing concentrations of FBP (●) or Serine (○). For **a** and **e-h**, the signal was normalised to controls containing no enzyme. The basal activity of the studied PK in each panel in the presence of vehicle control is indicated by the dotted line. Data are presented as mean \pm s.e.m. of duplicate determinations and are representative of three independent experiments.